Tuberculosis 96 (2016) 141–149

Contents lists available at ScienceDirect

Tuberculosis

journal homepage: http://intl.elsevierhealth.com/journals/tube

MODEL SYSTEMS

Route of delivery to the airway influences the distribution of pulmonary disease but not the outcome of *Mycobacterium tuberculosis* infection in rhesus macaques

Laura Sibley [a], Mike Dennis [a], Charlotte Sarfas [a], Andrew White [a], Simon Clark [a], Fergus Gleeson [b], Anthony McIntyre [b], Emma Rayner [a], Geoffrey Pearson [a], Ann Williams [a], Philip Marsh [a], Sally Sharpe [a, *]

[a] National Infection Service, Public Health England, Porton Down, Wiltshire, UK
[b] The Churchill Hospital, Headington, Oxford, UK

ARTICLE INFO

Article history:
Received 15 September 2015
Received in revised form
13 November 2015
Accepted 17 November 2015

Keywords:
Tuberculosis
Non-human primate
Challenge route
Immune response

SUMMARY

Non-human primates (NHP) provide a key component in the preclinical assessment pathway for new TB vaccines. In the established models, *Mycobacterium tuberculosis* challenge is typically delivered to airways of macaques either by aerosol or bronchoscopic instillation and therefore, an understanding of these delivery routes would facilitate the comparison of data generated from models using different challenge methods. This study compared the clinical effects, antigen-specific IFNγ response profiles and disease burden following delivery of comparable doses of *M. tuberculosis* to the lungs of rhesus macaques by either aerosol or bronchoscopic instillation. The outcome of infection in terms of clinical effects and overall disease burden was comparable between both routes of challenge. However, the pathology in the lungs differed as disease was localised to the site of inoculation following bronchoscopic instillation while aerosol exposure resulted in lesions being evenly distributed through the lung. Whilst the IFNγ response to PPD was similar, responses to CFP10 and ESAT6 peptide pools measured with an *ex vivo* ELISPOT differed with regards to responses to the N-terminal regions depending on the route of infection. Both challenge routes therefore provide valid and comparable models for evaluation of new TB vaccines, although subtle differences in host responses may occur.

1. Introduction

Tuberculosis (TB) continues to infect around 9 million people annually and was responsible for almost 1.5 million deaths worldwide in 2013 [1]. Although drug treatments are available and effective against active disease, the regimens are long (around 6 months) and have unpleasant side effects, which lead to non-compliance which in turn has contributed to the emergence of multidrug resistant (MDR) and extremely drug resistant (XDR) TB. There is a licensed vaccine available for TB; Bacille Calmette-Guerin (BCG), but it has variable efficacy depending on recipient age and geographical location, but it is effective in preventing serious disease in children [2,3].

There is therefore an urgent need for novel vaccines and therapeutics to prevent and control TB. One of the bottlenecks in the development of new interventions against TB is the lack of any identified correlates of protection, which means the only means of testing efficacy is by expensive, large scale clinical trials [4]. Therefore, preclinical animal models that can accurately predict the effectiveness of vaccines in humans through challenge studies are critical to identifying an improved TB vaccine. A range of species including mice, guinea pigs, rabbits and non-human primates (NHP) are used to model human tuberculosis [5]. NHPs provide the most relevant model of tuberculosis due to their similarity to humans [6–8], and reviews of published studies using the TB NHP model reveal that the selection of model parameters, including the macaque species, challenge route and size of the challenge dose, can affect the outcome of experimental TB exposure in NHPs [6–8]. The importance of route of *Mycobacterium tuberculosis* administration can be observed clearly in the murine

* Corresponding author. National Infection Service, Public Health England, Porton Down, Wiltshire, SP4 0JG, UK. Tel.: +44 1980 612811.
E-mail address: Sally.Sharpe@phe.gov.uk (S. Sharpe).

http://dx.doi.org/10.1016/j.tube.2015.11.004

model where mice have been reported to be more susceptible to infection by the aerosol route than by intravenous administration [9].

M. tuberculosis challenge is typically delivered to airways of macaques either by aerosol, intratracheal, intranasal or bronchoscopic instillation [8]. Aerosol exposure and bronchoscopic instillation cause granulomatous disease and an *M. tuberculosis* antigen-specific IFNγ response, both of which are characteristic features of TB disease [10,11]. Differences in pulmonary disease distribution have been reported as, following bronchoscopic instillation, disease is primarily localised to the site of inoculation in the lung, whereas aerosol exposure results in disease evenly distributed throughout the lung [12,13], as well as potential differences observed in rates of disease progression and dissemination to extra-pulmonary tissues.

The immune response is important to assess in vaccine evaluation studies in animal models to attempt to predict efficacy and immunogenicity. In humans, the immune response to TB is characterised by activation of Th1 T-cells and production of proinflammatory cytokines including IFNγ, TNFα, and IL-2 [14,15]. IFNγ production in response to CFP10 and ESAT6 as measured using an *ex vivo* ELISPOT assay is detected in naturally infected humans [16] as well as primates after aerosol and bronchoscopic instillation [10,11].

In order to provide the most clinically relevant and refined models for assessment of new TB therapeutics, it is important to determine the impact of challenge route on infection outcome, including the immune response. To date, a comparison of challenge routes in the same macaque species with the same *M. tuberculosis* strain and challenge dose has not been reported. The present study was set up to characterise the outcome of infection with an equivalent dose of *M. tuberculosis* delivered to rhesus macaques either by aerosol exposure or bronchoscopic instillation. In addition, the immune response profiles induced and the severity of the resulting disease between the two routes were compared in order to determine the impact that challenge route may have in future vaccine evaluation studies using macaque models.

2. Materials and methods

2.1. Experimental animals

Four male rhesus macaque of Indian genotype, aged 3–4 years were obtained from an established UK breeding colony for this study. Absence of previous exposure to mycobacterial antigens was confirmed by screening using an *ex vivo* IFN-γ ELISPOT (MabTech, Nacka. Sweden) to measure responses to PPD (SSI, Copenhagen, Denmark), and pooled 15-mer peptides of ESAT6 and CFP10 (Peptide Protein Research LTD, Fareham, U.K.).

Animals were housed in compatible social groups, in accordance with the Home Office (UK) Code of Practice for the housing and Care of Animals Bred, Supplied or Used for Scientific Purposes, December 2014, and the National Committee for Refinement, Reduction and Replacement (NC3Rs), Guidelines on Primate Accommodation, Care and Use, August 2006 (NC3Rs, 2006). Animals were sedated by intramuscular (IM) injection with ketamine hydrochloride (Ketaset, 100 mg/ml, Fort Dodge Animal Health Ltd, Southampton, UK; 10 mg/kg) for procedures requiring removal from their housing. None of the animals had been used previously for experimental procedures. All animal procedures were approved by the Public Health England Ethical Review Committee, Porton Down, UK, and authorized under an appropriate UK Home Office project license.

2.2. Clinical procedures

Animals were monitored daily for behavioural and clinical changes. Behaviour was evaluated for contra-indicators including depression, withdrawal from the group, aggression, changes in feeding patterns, respiration rate and coughing. Prior to blood sample collection, aerosol challenge and euthanasia, animals were weighed, body temperature measured and examined for gross abnormalities. Red blood cell (RBC) haemoglobin levels were measured using a HaemaCue haemoglobinometer (Haemacue Ltd, Dronfield, UK) to identify the presence of anaemia, and erythrocyte sedimentation rates (ESR) were measured using the Sediplast system (Guest Medical, Edenbridge, UK) to detect and monitor inflammation induced by infection with *M. tuberculosis*.

The time of necropsy, if prior to the end of the planned study period, was determined by experienced primatology staff and based on a combination of the following adverse indicators: depressed or withdrawn behaviour, abnormal respiration (dyspnoea), loss of 20% of peak post–challenge weight, ESR levels elevated above normal (>20 mm), haemoglobin level below normal limits (<100 g/dL), increased temperature (>41 °C) and abnormal chest X-ray or computed tomography scan.

2.3. M. tuberculosis challenge strain

The bacterial suspension used for challenge was prepared from stocks of the *M. tuberculosis* Erdman strain K 01 (BEI Resources). A stock suspension was initially prepared from a 5 ml bacterial starter culture originally generated from colonies grown on Middlebrook 7H11 supplemented with oleic acid, albumin, dextrose and catalase (OADC) selective agar (BioMerieux, UK). A liquid batch culture was then grown to logarithmic growth phase in 7H9 medium (Sigma–Aldrich, UK) supplemented with 0.05% (v/v) Tween80 (Sigma–Aldrich, UK). Aliquots were stored at −80 °C. The titre of the stock suspension was determined from thawed aliquots by enumeration of colony forming units cultured onto Middlebrook 7H11 OADC selective agar. The stock of Erdman was stored at a concentration of 1.1×10^8 CFU/ml.

2.4. Aerosol exposure

The methodology and apparatus used to deliver *M. tuberculosis* via the aerosol route was as previously described [11]. In brief, mono-dispersed bacteria in particles were generated using a 3-jet Collison nebuliser (BGI) and, in conjunction with a modified Henderson apparatus [17], delivered to the nares of each sedated primate via a modified veterinary anaesthesia mask. Challenge was performed on sedated animals placed within a 'head-out', plethysmography chamber (Buxco, Wilmington, North Carolina, USA) to enable the aerosol to be delivered simultaneously with the measurement of respired volume. The aerosol delivery process was designed to result in the deposition of a target dose of 35 CFU in the lungs. The number of bacilli deposited and retained in the lungs of macaques cannot be measured directly and the quantification of the dose must be calculated from the concentration of viable organisms in the aerosol (C_{aero}) and the volume of aerosol inhaled by the animal. This 'presented dose' (PD) is the number of organisms that the animals inhale. C_{aero} is either measured directly using air sampling within the system or may be calculated using the concentration of organisms in the nebulizer (C_{neb}) and a 'spray factor' which is a constant derived from data generated for the specific organism with identical aerosol exposure parameters. The calculations to derive the PD and the retained dose (the number of organisms assumed to be retained in the lung) have been described previously for high/medium aerosol doses [11,18,19]. The assumed

retained dose is calculated from the PD by applying a retention factor. Retention factors for rhesus macaques are described by Harper and Moreton [20] but a refinement of the retention factor for *M. tuberculosis* infections has been derived from cumulative data relating the PD to the number of lesions that have developed three weeks after challenge measured by CT.

2.5. Bronchoscopic instillation

The bacterial inoculum for intrabronchial delivery was prepared by dilution of an aliquot from the same suspension used for aerosol challenge into sterile PBS that provided a suspension whereby 2 ml contained approximately 35 CFU, which was verified by retrospective analysis. Each subject was anaesthetised with an intramuscular injection of a combination of ketamine hydrochloride (10 mg/kg. Anesketin, Eurovet Clinical Health, Bladel, The Netherlands), and medetomidine hydrochloride (50 ug/kg Sedator, Eurovet Clinical Health, Bladel, The Netherlands), and placed in ventral recumbency. The vocal chords were visualised using a laryngoscope and were sprayed with 2% w/v lignocaine hydrochloride (Intubeaze, Dechra Veterinary Products, Shrewsbury, UK) prior to insertion of a pre-sterilised bronchoscope (Allscope XE30 4-mm flexible bronchoscope; VES, Essex, UK). After insertion into the trachea, the bronchoscope was manoeuvred through the right bronchus into the right lower lung lobe and 2 ml of bacterial suspension was injected. Full distribution of the inoculum was ensured by subsequent delivery of 2 ml sterile saline, followed by 5 ml air.

2.6. Computed tomography (CT) imaging

CT scans were collected from animals using a 16 slice Lightspeed CT scanner (General Electric Healthcare, Milwaukee, WI, USA) as described previously [19,21]. In order to enhance visualisation of lesions and lymph nodes, Niopam 300 (Bracco, Milan, Italy), a non-ionic, iodinated contrast medium, was administered intravenously (IV) at 2 ml/kg body weight. Scans were evaluated for the number and distribution of pulmonary lesions across lung lobes and the presence of characteristic features of TB disease, for example: nodule cavitation, conglomeration and consolidation as an indicator of alveolar pneumonia and a 'tree-in–bud' pattern as an indicator of bronchocentric pneumonia. The lung-associated lymph nodes were assessed for enlargement and the presence of necrosis.

2.7. Immunological analysis

An ELISPOT assay was applied to measure the frequency of *M. tuberculosis* antigen-specific IFNγ producing cells in PBMC using an NHP cross-reactive human IFNγ kit (Mabtech, Sweden) according to the manufacturer's instructions. PBMC were isolated using Ficoll–Paque Plus (GE Healthcare, UK) using standard procedures. 2×10^5 and 1×10^5 PBMC were incubated with either medium (RPMI supplemented with Hepes buffer, Penicillin/Streptomycin, L-glutamine, 2-mercaptoethanol (all Sigma–Aldrich, UK) and 5% foetal calf serum (FCS, Labtech)), PPD (10 μg/ml) (Statens Serum Institute, Denmark) or peptide pools of CFP10 or ESAT6 at 37 °C 5% CO_2 overnight. Peptide pools were comprised of overlapping 15 mer peptides from peptidesynthetics (UK) used at a concentration of 50 μg/ml for each CFP10 and ESAT6 pool. Plates were analysed using a CTL Immunospot S6 reader and software (Bonn, Germany). Spot forming units (SFU) per million cells were calculated from the antigen stimulated wells minus the media only wells. Area under the curve (AUC) was calculated using GraphPad Prism software (v6) for Windows (La Jolla California, USA).

2.8. Necropsy

Animals were anaesthetised and clinical data collected. Blood samples were taken prior to euthanasia by intra-cardiac injection of a lethal dose of anaesthetic (Dolelethal, Vétoquinol UK Ltd, 140 mg/kg). A post-mortem examination was performed immediately and gross pathological changes were scored using an established system based on the number and extent of lesions present in the lungs, spleen, liver, kidney and lymph nodes; described previously [10].

2.9. Histopathological examination

Representative samples from each lung lobe (seven per animal) and other organs, were processed to paraffin wax, sectioned at 3–5 μm and stained with haematoxylin and eosin (HE). For each lung lobe, tissue slices containing obvious lesions were chosen for histological examination. Where gross lesions were not visible, a sample was taken from a pre-defined anatomical location from each lobe to establish consistency between animals. Sections of lung-associated lymph nodes (trachea-bronchial at the bifurcation and cranial and caudal to the bifurcation) and other tissues were evaluated for the presence of tuberculous lesions. Lesions in the lung parenchyma were identified, categorised and counted as described previously [19]. Briefly, lesions defined as "unorganised" (Types 1–3) were those lacking a peripheral cuff of lymphocytes, while "organised" lesions were those with a cuff of lymphocytes (Types 4 and 5). Classic largely well demarcated granulomas with central, caseous necrosis and a variable rim of lymphocytes, were classified as Type 6 lesions in line with studies by Kaushel et al. [6], and Lin et al., [10]. In one HE stained section from each lung lobe, granulomas types, as described above were counted and recorded. Further features included coalescing lesions, cavity formation and fulminating pneumonia, the latter defined as representing inflammatory changes within the parenchyma, extending between granulomas were recorded, together with additional, morphological features: airway invasion, lymphatic inflammation/involvement, arterial wall infiltration by inflammatory cells and granulomas in bronchovascular, connective tissue.

2.10. Bacteriology

The spleen, kidneys, liver and tracheobronchial lymph nodes were sampled for the presence of viable *M. tuberculosis* post-mortem as described previously [10]. Weighed tissue samples were homogenized in 2 ml of sterile water, then either serially diluted in sterile water prior to being plated, or plated directly onto Middlebrook 7H11 OADC selective agar. Plates were incubated for 3 weeks at 37 °C and resultant colonies were confirmed as *M. tuberculosis* and counted.

3. Results

3.1. Delivery of equivalent doses of M. tuberculosis by aerosol or bronchoscope

Doses of *M. tuberculosis* delivered by aerosol were of similar magnitude to those delivered by bronchoscope. The culture of samples collected during aerosol delivery confirmed that the two macaques were exposed to presented doses of 115 CFU (U45) or 122 CFU (U75), respectively, which were calculated to result in estimated doses of 29 CFU (U45) or 31 CFU (U75) retained in the lungs. Similarly culture of samples collected during the preparation of the suspension delivered by bronchoscopy quantified the dose delivered to the lungs at 29 CFU.

3.2. Clinical assessment post exposure

The disease progression was similar between the *M. tuberculosis* challenge routes (Figure 1A). Following exposure to *M. tuberculosis*, the macaques were monitored daily for changes in behaviour and every two weeks for changes in clinical parameters for 20 weeks after challenge. All four animals showed changes in behaviour and clinical parameters consistent with tuberculosis infection, including weight loss (Figure 1B), increased ESR (Figure 1) and reduction in red blood cell haemoglobin level (Figure 1D). Cough was observed and respiration rates were seen to become more rapid. Disease progressed to a level that met the humane endpoint criteria in one animal that received challenge by the aerosol route (U75, peak post challenge body weight loss: 17%, ESR: 42 mm, RBC [Hb]: 96 g/dL) at week 10, and one animal that was challenged by bronchoscopic instillation (U9, peak post challenge body weight loss: 20.8%, ESR: 79 mm, RBC[Hb]: 97 g/dL). At the end of the planned 20 week study period (Figure 1D), both the remaining animals were euthanized. The clinical parameters measured on the day of euthanasia of the animal that was challenged by bronchoscopic instillation (U64) reached endpoint criteria (peak post challenge body weight loss: 24.9%, ESR: 25 mm, RBC[Hb]: 105 g/dL), while those measured in the animal that received challenge by the aerosol route (U45) remained within the normal ranges for the species (peak post challenge body weight loss: 2.1%, ESR: 1 mm, RBC[Hb]: 126 g/dL).

3.3. CT evaluation of pulmonary disease

The CT scans collected at three and eight weeks after exposure to *M. tuberculosis* revealed differences in the pattern of pulmonary disease that were characteristic for the route of administration (Table 1). Aerosol exposure led to the development of discrete nodules in multiple lobes in both animals (U45, U75), and the number of nodules increased between three (30 and 43) and eight (37 and 71) weeks after challenge (Figure 2A and B). One aerosol-exposed animal (U75) showed evidence of pneumonia with areas of consolidation present in the right and left lower lobes three weeks after challenge, and both aerosol-exposed animals possessed consolidated areas in all lobes by eight weeks. Furthermore, eight weeks after challenge, U75 had also developed a cavity in the right upper lobe, and the middle lobe had become partially necrotic. Three weeks after intrabronchial inoculation, discrete nodules (10 and 5) were only seen in the right lower lobe in both animals (U9, U64) (Figure 2C) and by week eight it was no longer possible to identify discrete nodules in the lung (Figure 2D). Consolidation was only detected in the right lower lobe in both animals three weeks after bronchoscopic inoculation, and this had become extensive by eight weeks. Scans from both animals at week eight showed the radiological feature of ground glass opacification in the middle lobe, caused by the thickening of alveolar walls, or the presence of cells or fluid filling the alveolar spaces which can represent active disease, such as pulmonary oedema, pneumonia, or diffuse alveolar damage. Additionally, one animal (U9) had developed a cavity in the right lower lobe and the other (U64) showed evidence of necrosis in the same lobe, as well as collapse of the left lower lobe due to compression of the lower lobe bronchus by enlarged lymph nodes.

Enlarged tracheobronchial lymph nodes were detected in one (U75) of the two aerosol-exposed animals and both of the intrabronchially inoculated animals at both three and eight weeks after challenge. Evidence of necrosis was seen in subcarinal lymph nodes of the intrabronchially inoculated animal U9 at week three, and in both the intrabronchially inoculated animals and the aerosol-exposed animal, U75, at week eight after challenge. The right supraclavicular fossa lymph nodes appeared enlarged and necrotic in both the animals that received intrabronchial inoculation when analysed eight weeks after challenge, but were not detected in the scans from either of the aerosol-exposed animals. Splenic abscesses were reported in U9 eight weeks after intrabronchial inoculation. Extra-pulmonary disease was not identified from the CT scans of the other three animals.

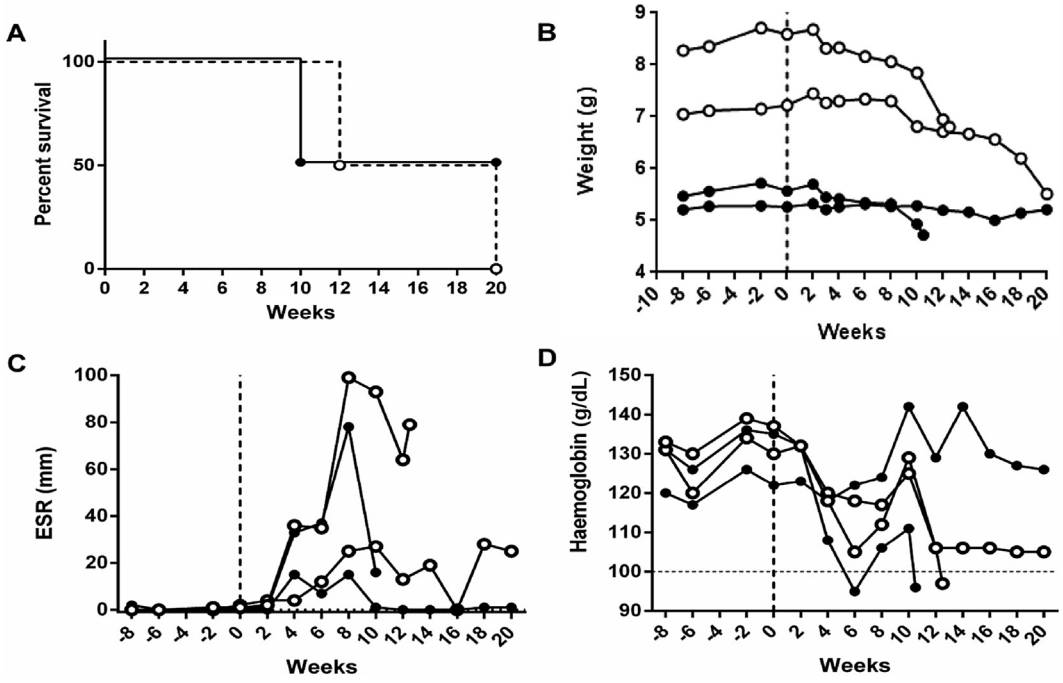

Figure 1. Clinical profiles from rhesus macaques infected with *M. tuberculosis* either by the aerosol route or by bronchoscopic instillation. Open symbols; bronchoscopic instillation, closed symbols; aerosol. A) Survival plot, B) Total body weight, C) Erythrocyte sedimentation rate (ESR), D) Haemoglobin level.

Table 1
Summary of CT findings.

	Aerosol	Bronchoscopic instillation
Lung		
Discrete pulmonary nodules	Evenly distributed through lobes Number of discrete lesions increased over time	Restricted to lower right lobe at week 3 Not countable as individual lesions due to consolidation/conglomeration by week 8
Pneumonia	Areas of consolidation in all lung lobes and weeks 3 and 6	Consolidation in the lower right lobe of both animals at week 3 and 8 Ground glass opacification in middle right lobe of both animals at week 8 – evidence of intra-bronchial spread?
Cavitation	One animal, right upper lobe	One animal, right lower lobe
Other features		One animal left lower lobe collapse due to lymph node compression
Tracheobronchial LN		
Enlargement	LNs seen in one animal at week 3 and 8	LNs seen in both at weeks 3 and 8 Right Supraclavicular fossa node enlargement in both
Necrotic sub-carinal LN	Neither at week 3, but 1 at week 8	One at week 3 and both at week 8
Extra-pulmonary disease	Neither	One animal displayed splenic abscesses

3.4. Evaluation of disease burden post-mortem

Disease burden was evaluated during a *post-mortem* examination conducted at the point at which disease progressed to a level that met the humane endpoint criteria in three animals at weeks 10 (U75), 12 (U9) and 20 (U64) after challenge, and at the end of the planned study period (week 20) for the remaining animal (U45). The total gross pathology scores obtained from the pair of aerosol-exposed animals (55, 81) were equivalent to the scores from the pair of intrabronchially-challenged animals (60, 81) (Figure 3A). Closer evaluation of the break-down of the total score revealed subtle differences between the disease resulting from the two delivery routes (Figure 3B and C). The scores from the left lung lobes were larger in the aerosol-exposed animals (lower lobe scores, aerosol group: 5 and 8, intrabronchial group: 3 and 4; upper lobe score, aerosol group 7 and 9, intrabronchial group: 4 and 4); by contrast, the intrabronchially challenged animals showed a larger disease score associated with the paratracheal lymph nodes (Intrabronchial group scores: 2 and 6; Aerosol group scores: 0 and 1).

Following necropsy, MR images of the lungs of each animal were collected [11,19,23]. Images from each sequential tissue slice were reconstructed into three-dimensional images of the entire lung using computer software for all study subjects. Representative images from animals that were exposed by the two different routes to *M. tuberculosis* are shown in Figure 3D and E. The lesions were

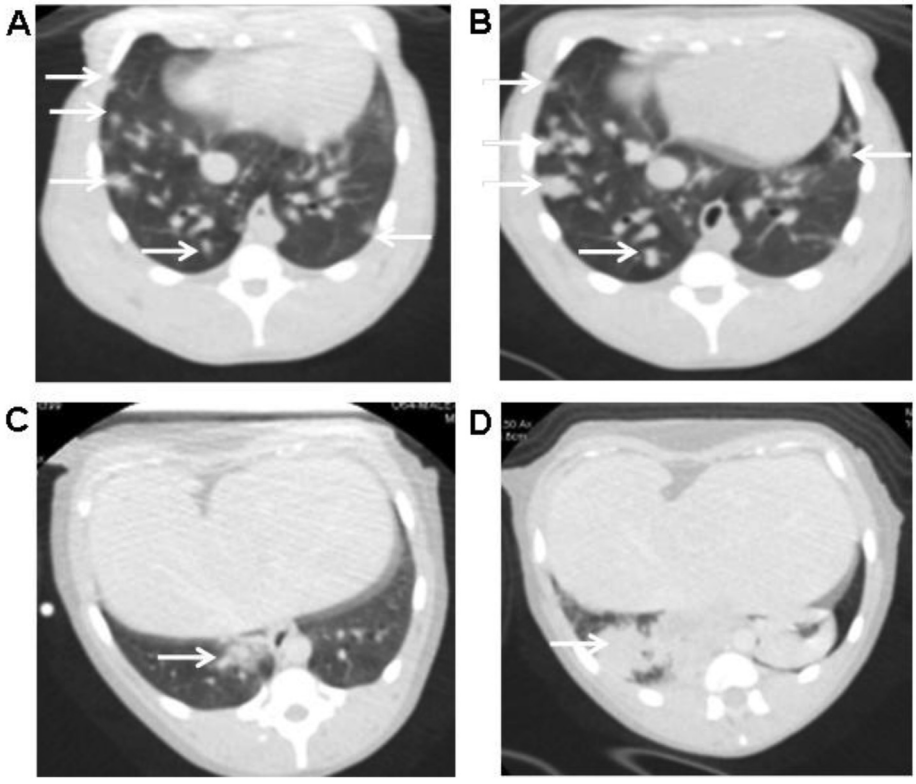

Figure 2. CT *in vivo* images of lungs of rhesus macaques infected with *M. tuberculosis* by either aerosol exposure or bronchoscopic instillation. The CT images demonstrate the difference in number and distribution of focal areas of infection, arrowed, secondary to the different techniques of administration of TB. A) Representative aerosol infected animal, week 3, B) Representative aerosol infected animal, week 8, C) Representative bronchoscopic instillation infection at week 3, D) Representative bronchoscopic instillation infection at week 8.

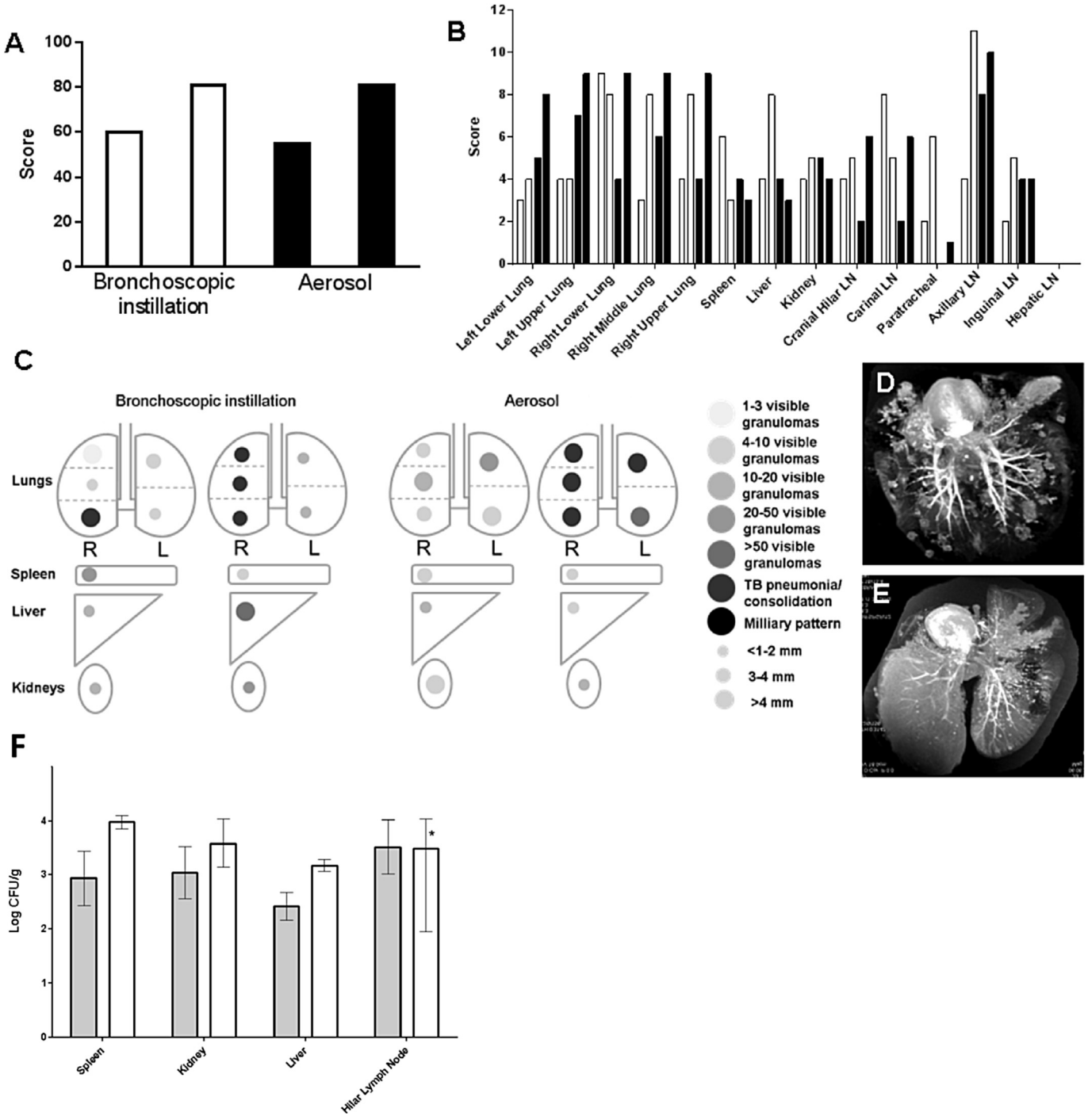

Figure 3. Disease burden pathology readouts from rhesus macaques infected with *M. tuberculosis* either by the aerosol route or by bronchoscopic instillation. A) Total pathology scores, B) breakdown of pathology score for each tissue, C) diagrams illustrating the pathology scores for the lungs, spleen, liver and kidneys after bronchoscopic instillation or aerosol dosing. Greyscale indicates number and size of lesions. Panels D and E represent *ex vivo* MRI images of the lungs. D) Aerosol infected E) bronchoscopic instillation. The volumetric MRI shows the widespread multi lobar infection following aerosol administration (D) compared to the almost unilobar distribution following intrabronchial administration (E). F. Bacterial burden in extra-pulmonary tissues and hilar lymph nodes, * below limit of detection (1.95 $\log_{10}$ CFU/g) in one animal.

evenly distributed throughout all of the lobes of the lung following aerosol exposure (Figure 3D), while intrabronchial placement led to a more focal disease on the right side of the lung with an increased level of endobronchial involvement (Figure 3E). The disease at the site of intrabronchial inoculation appeared to be more severe compared to the level in any of the lung lobes after aerosol exposure.

Evaluation of the microscopic pathology of the lung did not detect obvious microscopic differences between animals and groups. Microscopic lesions attributable to (or consistent with) infection with *M. tuberculosis* (Mtb) were observed in all the lung lobes in all animals in both groups. Granulomas classified as Types 5 and 6, were the most prevalent, many of which were coalescing. Granulomas of Types 1 to 4 were observed at variable levels

between lung lobes and between animals. Cavity lesions were seen in two animals [U9 (intra-bronchial) and U45 (aerosol)]. Airway involvement was observed in all animals, being most prominent in animals U9 (intra-bronchial) and U45 (aerosol). However, with respect to airway invasion, it was recognised that in three animals, U45 and U75 (aerosol challenge) and U9 (intra-bronchial challenge), the right and left sides of the lung were equally affected. In animal U64, airway invasion was only seen in the right middle and lower lung lobes. In addition, perivascular, lymphoid cuffing; lymphatic inflammation/involvement; vascular (mainly arterial) wall infiltration by inflammatory cells were occasionally recorded, and giant cells, sometimes bizarre, were frequently seen. In all animals, tracheobronchial lymph nodes were enlarged and largely replaced by granulomatous lesions with caseous necrosis and occasional calcification. Microscopic granulomas were detected in tracheobronchial lymph nodes of all animals. In the two animals in the intra-bronchial challenge group, tuberculous lesions were detected in lymph nodes distant from the lungs, U64 (right axillary lymph node) and U9 (right inguinal, hepatic and thoracic lymph nodes). In the aerosol challenge group, lesions were not observed in the lymph nodes other than the pulmonary nodes. A range of tuberculous granulomas from small granulomatous lesions to large, caseating lesions were observed in the livers of all four animals and, similarly, granulomatous lesions of variable size were seen in both left and right kidneys of all four animals. Examination of the spleen revealed typical, caseous, tubercular lesions in three animals [U9, U64 (intra-bronchial challenge) and U75 (aerosol challenge)] but lesions were not observed in animal U45. In two animals, U9 (intra-bronchial challenge) and U75 (aerosol challenge), parietal pleural involvement (thoracic cavity) with tuberculous lesions was seen.

3.5. Extra-pulmonary organ-specific bacterial burden

The bacterial burden was evaluated in the liver, spleen, kidneys, hilar lymph nodes, blood and urine for all animals. *M. tuberculosis* was isolated from the spleen, kidneys, and liver from all four animals and the hilar lymph nodes from both of the aerosol challenged animals (U45, U75) and one of the intrabronchially challenged animals (U9). The mean values (CFU/g) for each route of infection across each of the tissue types are shown in Figure 3F and the value for each of the pair of animals is indicated by the range bars. No bacteria were recovered from the hilar lymph node of animal U64 but only a small tissue sample (0.11 g) was available for assessment. For this animal the value given is 0.5× the limit of detection (1.95 $\log_{10}$ CFU/g). A similar level of bacterial burden was seen between the animals and between the delivery routes, indicating a similar distribution of extra-pulmonary dissemination with both routes of infection. *M. tuberculosis* was not cultured at detectable levels from the blood or urine from any of the four animals.

3.6. Immunological analysis

An *ex vivo* ELISPOT assay was used to measure the *M. tuberculosis*-specific IFNγ response at two weekly intervals over 20 weeks following challenge (Figure 4) by assessing responses to the TB antigens PPD and overlapping 15 mer peptides of CFP10 and ESAT6 arranged into three pools (A, B and C). All animals, irrespective of challenge route, made a high PPD-specific response to infection with similar kinetics (Figure 4A). High responses were also seen to CFP10 and ESAT6 summed peptide pools (Figure 4B and C). Area under the curve (AUC) analysis of the CFP10 response measured as sum of SFU to peptide pools A, B, and C suggested a trend for higher responses in the intrabronchially challenged animals (Figure 4J). Similar examination of the responses made to the individual peptide pools revealed CFP10 peptide pool A stimulated a response in the macaques which received *M. tuberculosis* by bronchoscope that was five times greater than the mean response observed in the macaques exposed by aerosol (Figure 4K). The opposite trend was observed with CFP10 peptide pool B, where the aerosol challenged animals showed a higher response to the peptide pool (Figure 4K). The responses to CFP10 pool C were not markedly different between the two challenge routes (Figure 4K). A high, early response to ESAT6 predominantly against peptide pool A was seen in the aerosol exposed animals that was not seen in the animals that received *M. tuberculosis* by bronchoscope (Figure 4G). For ESAT6 peptide pools B, the initial kinetics were similar between challenge routes (Figure 4H) but the overall AUC analysis showed that the response was higher in the bronchoscopic instillation group (Figure 4L), which can be attributed to a longer lasting response in this group. In ESAT6 peptide pool C, the challenge routes showed similar responses between challenge routes (Figure 4I and L).

4. Discussion

Although aerosol is the natural route of TB transmission, many vaccine efficacy evaluations are performed in macaque models that use the bronchial route for challenge because of technical expediency. Speculation exists as to whether the outcome is equivalent when either delivery route for challenge is used, and to date there have been no head-to-head comparisons. The aim of this study was to evaluate the outcome of *M. tuberculosis* infection in rhesus macaques following delivery of equivalent doses to the lung by aerosol or by bronchoscopy. As NHP models provide a key component in the preclinical assessment pathway for new TB vaccines, and will become increasingly important as a gateway to clinical trials [22], an understanding of the impact of using intra-bronchial or aerosol delivery needs to be determined to enable the comparison of data generated from models using different challenge routes.

The challenge doses of *M. tuberculosis* delivered for this study were comparable in terms of the estimated retained dose. The small variation in the calculated doses is a reflection of the technical challenges associated with delivery, the calculation of the dose delivered and the estimation of the dose retained. Delivery of *M. tuberculosis* by aerosol or bronchoscope induced equivalent clinical outcomes, PPD-specific IFNγ response profiles, and overall disease burden including extra-pulmonary bacterial load and histological changes. Changes in clinical parameters, such as body weight, extra-pulmonary spread and gross pathology assessment scores are important measures of disease burden, that when compared between test and control groups in vaccine evaluation studies provide key indicators of protective efficacy. The indications from this study suggest that the outcome of vaccine evaluation assessments based on these readouts, using either route of *M. tuberculosis* delivery, would be equally capable of revealing new vaccines with good protective potential. Candidate vaccines would not be disadvantaged by the method of challenge delivery used in the NHP model selected for the assessment. Further work using a larger group of animals will be required to confirm the comparability of these readouts between intrabronchial and aerosol delivery models and their utility as cross model comparators.

Although the effect on the host resulting from the two delivery routes appeared to be equivalent, differences were seen in the distribution of pulmonary disease induced following aerosol or bronchoscopic delivery; these differences were in line with those previously reported [12,13,23,24]. The disease which developed following inoculation by bronchoscope showed increased severity on the right side of the lung with changes being most severe in the right lower lobes, while aerosol exposure resulted in disease spread evenly through both sides of the lung. The targeted bronchoscopic

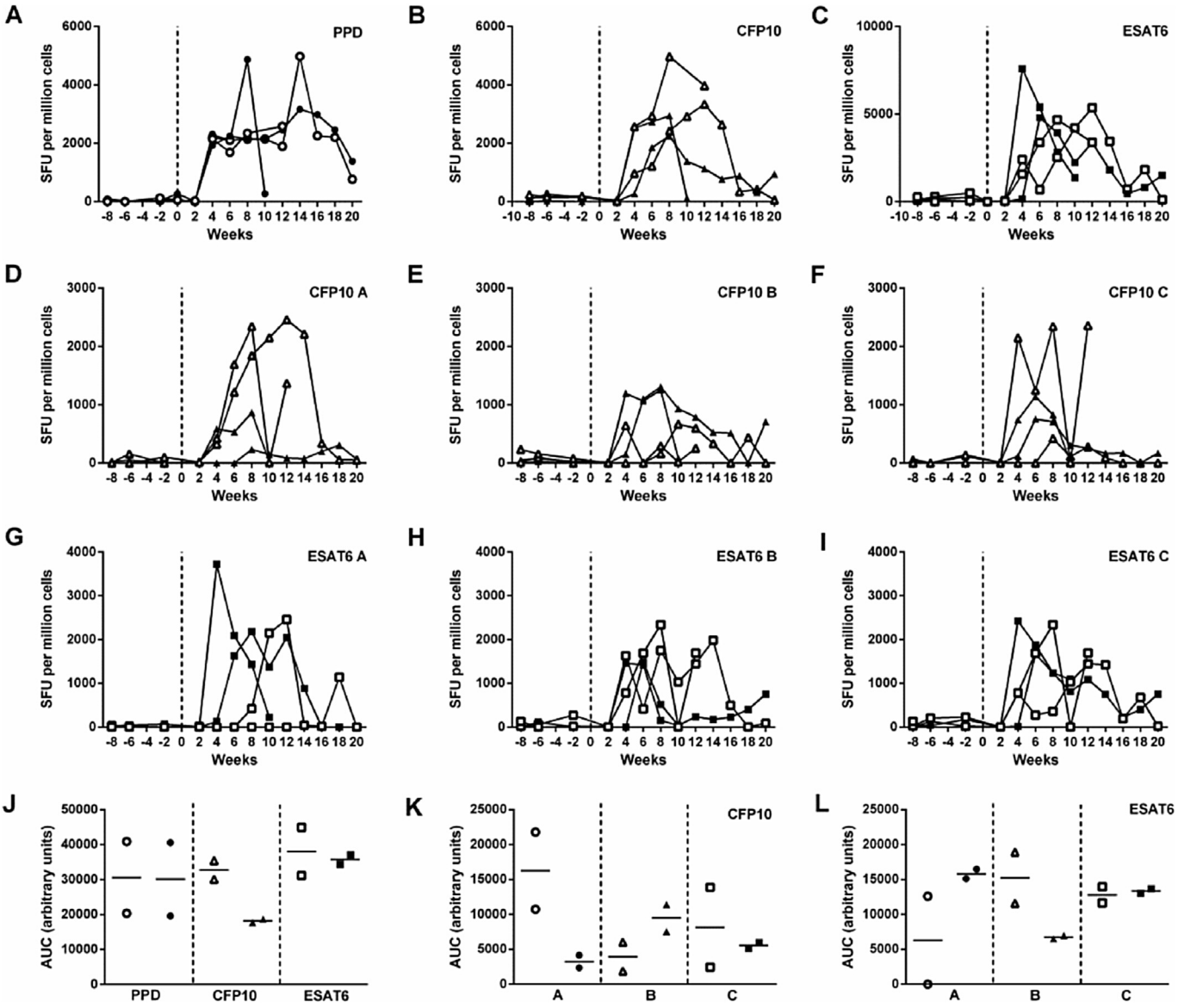

Figure 4. IFNγ ELISPOT responses to stimulation with PPD or CFP10 and ESAT6 peptide pools after aerosol or bronchoscopic instillation challenge with *M. tuberculosis*. IFNγ ELISPOT PBMC responses to stimulation over time from rhesus macaques challenged with *M. tuberculosis* by either bronchoscopic instillation (open symbols) or by aerosol (closed symbols). Dotted line indicates time of challenge with *M. tuberculosis*. A) Responses to PPD, B) responses to summed peptide pools of CFP10, C) responses to summed peptide pools of ESAT6. Panels D–I: IFNγ ELISPOT PBMC responses to stimulation with peptides pools over time D) CFP10 peptide pool A, E) CFP10 peptide pool B, F) CFP10 peptide pool C, G) ESAT6 peptide pool A, H) ESAT6 peptide pool B, I) ESAT6 peptide pool C. Panels J–L area under the curve analysis J) PPD and summed peptide pools of CFP10 and ESAT6, K) CFP10 summed peptide pools, L) ESAT6 summed peptide pools.

delivery and uneven spread of disease in the lung resulted in areas that showed either increased, equivalent or reduced levels of disease compared to that induced by aerosol delivery. In human TB infection, disease is heterogeneous among the population; disease in the lung can be one sided, or distributed throughout the tissue [25]. Therefore, despite the observed differences in lung pathology, both routes used for experimental infection gave rise to features that were characteristic of TB-induced disease human infection. Furthermore, the route of delivery did not influence the microscopic nature of the granulomas that developed in the lungs. Tuberculous lesions were identified in non-pulmonary lymph nodes of the animals that received intra-bronchial challenge, but were not observed in the equivalent lymph in the aerosol challenge group which may be suggestive of a more rapid dissemination and involvement of the lymph nodes although the small size of this study means firm conclusions cannot be drawn from these findings.

The variation in pulmonary disease arising from the two routes of delivery, however, may induce differences in the host response. In this study we used an *ex vivo* ELISPOT assay to evaluate the ESAT6 and CFP10-specific IFNγ responses to infection and, although animal numbers are small, some consistent differences were seen in the responses made by aerosol- or intrabronchially-challenged animals. The consistency of the responses made by each pair of animals that received *M. tuberculosis* by the same route, and the difference in the responses between groups of outbred NHPs, is noteworthy. The ESAT6 and CFP10 profiles observed in the group infected following aerosol exposure are similar to those reported in naturally-infected humans, which generally show immune responses to motifs found in the ESAT6 N-terminus and C-terminus (ESAT6 pools A, B and C) and CFP10 middle and C-terminus (CFP10 pools B and C) [16,26,27]. However the macaques infected by bronchoscopic instillation made an IFNγ response to CFP10 peptide

pool A, which corresponds to the CFP10 N-terminal region, which was shown by Arlehamn et al. to be only weakly immunogenic in humans [16]. Further studies using larger group sizes would be necessary to confirm these observations and evaluate the implications.

This study indicates that the delivery of comparable doses of *M. tuberculosis* to the lungs of rhesus macaques by either aerosol or bronchoscopy results in comparable outcomes. Therefore, both challenge routes for experimental infection of macaques provide valid models for evaluation of new TB vaccines. There may be some implications in terms of immune response to antigens that is a consequence of route of challenge, but further work is required to verify any differences.

Acknowledgements

This work was supported by The Gates Foundation and the Department of Health, UK. The views expressed in this publication are those of the authors and not necessarily those of the Department of Health. We thank the staff of the Biological Investigations Group at PHE Porton and the PHE macaque colonies for assistance in conducting studies; Tracy Benford and Faye Lanni for bacteriology and aerobiology support, and Donna Smyth for assistance with imaging.

Funding: This work was supported by The Gates Foundation and the Department of Health, UK.

Competing interests: None declared.

Ethical approval: All procedures described in this paper were conducted under the authority of a Home Office approved project licence that had undergone ethical review by the Institute's Animal Welfare and Ethical Review Body as required under the UK Animals(Scientific Procedure) Act, 1986.

References

[1] WHO. WHO|Tuberculosis. WHO; 2014. http://www.who.int/mediacentre/factsheets/fs104/en/ [accessed 04.08.14].
[2] Trunz BB, Fine P, Dye C. Effect of BCG vaccination on childhood tuberculous meningitis and miliary tuberculosis worldwide: a meta-analysis and assessment of cost-effectiveness. Lancet 2006;367:1173–80. http://dx.doi.org/10.1016/S0140-6736(06)68507-3.
[3] Zwerling A, Behr MA, Verma A, Brewer TF, Menzies D, Pai M. The BCG World Atlas: a database of global BCG vaccination policies and practices. PLoS Med 2011;8:e1001012. http://dx.doi.org/10.1371/journal.pmed.1001012.
[4] Tameris MD, Hatherill M, Landry BS, Scriba TJ, Snowden MA, Lockhart S, et al. Safety and efficacy of MVA85A, a new tuberculosis vaccine, in infants previously vaccinated with BCG: a randomised, placebo-controlled phase 2b trial. Lancet 2013;381:1021–8. http://dx.doi.org/10.1016/S0140-6736(13)60177-4.
[5] Gupta UD, Katoch VM. Animal models of tuberculosis. Tuberc (Edinb) 2005;85:277–93. http://dx.doi.org/10.1016/j.tube.2005.08.008.
[6] Kaushal D, Mehra S, Didier PJ, Lackner AA. The non-human primate model of tuberculosis. J Med Primatol 2012;41:191–201. http://dx.doi.org/10.1111/j.1600-0684.2012.00536.x.
[7] Scanga CA, Flynn JL. Modeling tuberculosis in nonhuman primates. Cold Spring Harb Perspect Med 2014;4:a018564. http://dx.doi.org/10.1101/cshperspect.a018564.
[8] Peña JC, Ho W-Z. Monkey models of tuberculosis: lessons learned. Infect Immun 2015;83:852–62. http://dx.doi.org/10.1128/IAI.02850-14.
[9] North RJ. Mycobacterium tuberculosis is strikingly more virulent for mice when given via the respiratory than via the intravenous route. J Infect Dis 1995;172:1550–3.
[10] Lin PL, Rodgers M, Smith L, Bigbee M, Myers A, Bigbee C, et al. Quantitative comparison of active and latent tuberculosis in the cynomolgus macaque model. Infect Immun 2009;77:4631–42. http://dx.doi.org/10.1128/IAI.00592-09.
[11] Sharpe SA, McShane H, Dennis MJ, Basaraba RJ, Gleeson F, Hall G, et al. Establishment of an aerosol challenge model of tuberculosis in rhesus macaques and an evaluation of endpoints for vaccine testing. Clin Vaccine Immunol 2010;17:1170–82. http://dx.doi.org/10.1128/CVI.00079-10.
[12] Lewinsohn DM, Tydeman IS, Frieder M, Grotzke JE, Lines RA, Ahmed S, et al. High resolution radiographic and fine immunologic definition of TB disease progression in the rhesus macaque. Microbes Infect 2006;8:2587–98. http://dx.doi.org/10.1016/j.micinf.2006.07.007.
[13] Lin PL, Coleman T, Carney JPJ, Lopresti BJ, Tomko J, Fillmore D, et al. Radiologic responses in cynomolgous macaques for assessing tuberculosis chemotherapy regimens. Antimicrob Agents Chemother 2013. http://dx.doi.org/10.1128/AAC.00277-13.
[14] Borgström E, Andersen P, Atterfelt F, Julander I, Källenius G, Maeurer M, et al. Immune responses to ESAT-6 and CFP-10 by FASCIA and multiplex technology for diagnosis of M. tuberculosis infection; IP-10 is a promising marker. PLoS One 2012;7:e43438. http://dx.doi.org/10.1371/journal.pone.0043438.
[15] Prezzemolo T, Guggino G, La Manna MP, Di Liberto D, Dieli F, Caccamo N. Functional signatures of human CD4 and CD8 T cell responses to Mycobacterium tuberculosis. Front Immunol 2014;5:180. http://dx.doi.org/10.3389/fimmu.2014.00180.
[16] Arlehamn CSL, Sidney J, Greenbaum JA, James EA, Moutaftsi M, Coler R, et al. Dissecting mechanisms of immunodominance to the common tuberculosis antigens ESAT-6, CFP10, Rv2031c (hspX), Rv2654c (TB7.7), and Rv1038c (EsxJ). J Immunol 2012;188:5020–31. http://dx.doi.org/10.4049/jimmunol.1103556.
[17] Druett HA. A mobile form of the Henderson apparatus. J Hyg (Lond) 1969;67:437–48.
[18] Clark SO, Hall Y, Kelly DLF, Hatch GJ, Williams A. Survival of Mycobacterium tuberculosis during experimental aerosolization and implications for aerosol challenge models. J Appl Microbiol 2011;111:350–9. http://dx.doi.org/10.1111/j.1365-2672.2011.05069.x.
[19] Rayner EL, Pearson GR, Hall GA, Gleeson F, McIntyre A, Smyth D, et al. Early lesions following aerosol challenge of rhesus macaques (Macaca mulatta) with Mycobacterium tuberculosis (Erdman strain). J Comp Pathol 2015;152:217–26. http://dx.doi.org/10.1016/j.jcpa.2014.10.002.
[20] Harper GJ, Morton JD. A method for measuring the retained dose in experiments on airborne infection. J Hyg (Lond) 1962;60:249–57.
[21] Dennis MJ, Parks S, Bell G, Taylor I, Lakeman J, Sharpe SA. A flexible approach to imaging in ABSL-3 laboratories. Appl Biosaf 2015;20.
[22] CTVD. BMGF TB vaccine strategy. 2015. https://www.ctvd.co/Pages/Strategy.aspx [accessed 08.09.15].
[23] Sharpe SA, Eschelbach E, Basaraba RJ, Gleeson F, Hall G, McIntyre A, et al. Determination of lesion volume by MRI and stereology in a macaque model of tuberculosis. Tuberculosis 2009;89:405–16. http://dx.doi.org/10.1016/j.tube.2009.09.002.
[24] Barclay WR, Anacker RL, Brehmer W, Leif W, Ribi E. Aerosol-induced tuberculosis in subhuman primates and the course of the disease after intravenous BCG vaccination. Infect Immun 1970;2:574–82.
[25] Jeong YJ, Lee KS. Pulmonary tuberculosis: up-to-date imaging and management. Am J Roentgenol 2008 Sep;191(3):834–44. http://dx.doi.org/10.2214/AJR.07.3896. http://www.ncbi.nlm.nih.gov/pubmed/18716117.
[26] Day CL, Moshi ND, Abrahams DA, van Rooyen M, O'rie T, de Kock M, et al. Patients with tuberculosis disease have Mycobacterium tuberculosis-specific CD8 T cells with a pro-apoptotic phenotype and impaired proliferative capacity, which is not restored following treatment. PLoS One 2014;9:e94949. http://dx.doi.org/10.1371/journal.pone.0094949.
[27] Ulrichs T, Munk ME, Mollenkopf H, Behr-Perst S, Colangeli R, Gennaro ML, et al. Differential T cell responses to Mycobacterium tuberculosis ESAT6 in tuberculosis patients and healthy donors. Eur J Immunol 1998;28:3949–58. http://dx.doi.org/10.1002/(SICI)1521-4141(199812)28. 12<3949::AID-IMMU3949>3.0.CO;2–4.